15 June 1996

ELSEVIER

Optics Communications 127 (1996) 230–236

OPTICS COMMUNICATIONS

Exact quantum theory of a parametrically driven dissipative anharmonic oscillator

G.Yu. Kryuchkyan *, K.V. Kheruntsyan

Institute for Physical Research, National Academy of Sciences of Armenia, 378410 Ashtarak-2, Armenia

Received 3 October 1995; accepted 7 December 1995

Abstract

We present an exact quantum theory of a model of a parametrically driven dissipative anharmonic oscillator. The model describes a Kerr interaction of an intracavity signal mode which is parametrically excited by a strong driving field via the process of frequency down conversion. Our analysis deals with the nonlinear treatment of light quantum fluctuations and hence allows to study qualitative effects in the transition from slightly perturbed classical behavior to a manifestly quantum mechanical behavior. We find an exact analytical steady-state solution of the Fokker–Planck equation in complex P-representation and calculate (i) normally ordered operator moments and (ii) the photon number probability distribution function of the generated signal field. The critical role of quantum noise in the nonlinear dynamics and in the quantum statistical properties of the signal field is demonstrated. The disappearance of characteristic threshold behavior is shown in the case of large nonlinearities or of increasing quantum noise strength. The ability of the nonlinear system to produce quadrature-squeezed and sub-Poissonian states is demonstrated as well.

1. Introduction

Nonlinear optical systems leading to the generation of nonclassical light are currently the subject of much theoretical and experimental attention in quantum optics. One of the central problems in this field of research is understanding the role of quantum noise in nonlinear dynamics and in the quantum statistical properties of generated light fields. In most theoretical works, however, the nonlinear systems are usually described within the linear treatment of light quantum fluctuations, i.e. they are considered to be only slightly perturbed from the classical behavior. It is clear that such an approach has a limited range of applications. In particular, it does not describe the behavior of nonlinear systems in critical (threshold, turning, instability, etc.) regions and in the case of quantum noise of arbitrary strength.

A more adequate description of quantum optical nonlinear systems can be achieved within the framework of an exact nonlinear treatment of quantum fluctuations via the solution of the Fokker–Planck equation for a quasiprobability distribution function. This approach gives the possibility to refine the results of linearized theories quantitatively, as well as to predict new qualitative phenomena. However, the derivation of quasiprobability distribution functions for realistic models of nonlinear interactions including dissipation effects is a difficult problem,

* Corresponding author. Fax: +7 8852 523640; E-mail: ifi@arminco.com.

PII S0030-4018(96)00021-1

which was solved for a few simple models (see, e.g., Refs. [1–6]). Among these models the most attractive and well-known ones are the degenerate parametric oscillator and anharmonic oscillator models [1,3,4,6–8]. They are responsible, in particular, for the process of intracavity parametric frequency down conversion and for nonlinear interaction in a Kerr medium leading to dispersive optical bistability, respectively. Many quantum optical predictions have been made using these nonlinear systems, and some of them have also been verified with experiments [1,4,6–15].

On the other hand, interesting results have been predicted recently for a model of a parametrically driven anharmonic oscillator [16,17]. This model can be formulated just as a combination of the usual parametric oscillator and of anharmonic oscillator models. Being applied to optics it can describe a Kerr interaction of a mode of an electromagnetic field which is parametrically driven in the process of frequency down conversion. Considering combinations of various nonlinear optical processes with Kerr interaction can lead to some advantages, in particular with respect to quantum optical effects and to new qualitative results [16,18–20]. It should be pointed out, however, that in Refs. [16,17] special cases were considered of a pulsed parametric oscillator combined with a Kerr nonlinearity and of a parametrically driven anharmonic oscillator without accounting for the effects of dissipation and quantum fluctuations.

It is the aim of this paper to present an exact quantum theory of a parametrically driven dissipative anharmonic oscillator. We find an exact steady-state solution of the Fokker–Planck equation in the complex P-representation. Using this solution we calculate analytically the normally ordered operator moments of the generated signal field and study the behavior of the signal field intensity, the second-order correlation function, the photon number and quadrature amplitude fluctuations, as well as the photon number probability distribution function.

2. Nonlinear system and Fokker–Planck equation

The nonlinear system under consideration combines $\chi^{(2)}$- and $\chi^{(3)}$-nonlinearities in a single-mode ring cavity of resonant frequency ω_c. The intracavity signal mode is excited via the $\chi^{(2)}$-nonlinear process of parametric frequency down conversion under the influence of a strong driving field at frequency ω (such that $\omega/2 \approx \omega_c$). Assuming single-pass effects in the driving field to be negligible, we employ the undepleted pump approximation and treat the amplitude of the driving field as a classical constant. In addition, we assume that the generated signal mode undergoes also a Kerr interaction, namely the self-phase modulation, due to the χ^3-nonlinearity. This nonlinear system can be modeled by the following effective interaction Hamiltonian:

$$H_{\text{eff}} = \frac{\hbar k}{2}\left(a^2 E^* \,\mathrm{e}^{\mathrm{i}\omega t} + a^{+2} E\,\mathrm{e}^{-\mathrm{i}\omega t}\right) + \frac{\hbar\chi}{4} a^{+2} a^2, \tag{1}$$

where a^+ and a are boson creation and annihilation operators of the signal mode ω_c, k and χ are coupling constants proportional to the second- and third-order susceptibilities $\chi^{(2)}$ and $\chi^{(3)}$, respectively, and E is the amplitude of the driving field.

Starting with the effective Hamiltonian (1) and accounting for the decay of the cavity mode we then use standard procedures [21,22] to obtain a master equation for the density operator of the signal mode in the interaction picture. Then we transform this master equation into a Fokker–Planck equation for the quasiprobability distribution function $P(\alpha, \beta)$ in the complex P-representation [2,21]. The resulting Fokker–Planck equation has the following form:

$$\begin{aligned}\frac{\partial P(\alpha,\beta)}{\partial t} &= \left\{ \frac{\partial}{\partial \alpha}\left[(\gamma - \mathrm{i}\Delta)\alpha + \mathrm{i}\frac{\chi}{2}\beta\alpha^2 + \mathrm{i}kE\beta \right] \right. \\ &\quad + \frac{\partial}{\partial \beta}\left[(\gamma + \mathrm{i}\Delta)\beta - \mathrm{i}\frac{\chi}{2}\alpha\beta^2 - \mathrm{i}kE^*\alpha \right] \\ &\quad + \frac{1}{2}\frac{\partial^2}{\partial \alpha^2}\left[-\mathrm{i}\left(KE + \frac{\chi}{2}\alpha^2 \right) \right] \\ &\quad \left. + \frac{1}{2}\frac{\partial^2}{\partial \beta^2}\left[\mathrm{i}\left(kE^* + \frac{\chi}{2}\beta^2 \right) \right] \right\} P(\alpha,\beta). \end{aligned} \tag{2}$$

Here $\Delta = \omega/2 - \omega_c$ is the cavity detuning, γ is the cavity damping constant, and we have neglected the thermal fluctuations. α and β are independent complex variables corresponding to the operators a and

a^+, such that the normally ordered operator moments are obtained via

$$\langle a^{+m}a^n\rangle = \int_C\int_{C'} \mathrm{d}\alpha\, \mathrm{d}\beta\, \alpha^n\beta^m P(\alpha,\beta), \qquad (3)$$

where C and C' are appropriate integration paths in the individual complex planes for α and β.

3. Semiclassical steady-state intensity

Before proceeding with the exact steady-state solution of the Fokker–Planck equation, we present the results of the analysis of stable semiclassical solutions α_0, β_0 ($\beta_0=\alpha_0^*$) for the amplitude of the signal mode. They can be easily obtained from stochastic differential equations [21] equivalent to (2) by dropping time derivatives and by ignoring the noise terms. This corresponds to setting the drift terms in Eq. (2) equal to zero. Carrying out also a standard stability analysis with respect to small fluctuations, we obtain that there exist two stable steady-state solutions with $\alpha_0=0$ and $\alpha_0\neq 0$, which describe the below-threshold and the above-threshold regimes of oscillations, respectively. In terms of the intensity $n_0=|\alpha_0|^2$ (in photon number units) and the phase φ_0 of the signal mode ($\alpha_0=n_0^{1/2}\exp(\mathrm{i}\varphi_0)$) the stable above-threshold solution is determined by the following expressions:

$$n_0=\frac{2\gamma}{\chi}\left[d+(J-1)^{1/2}\right], \qquad (4)$$

$$\sin(\Phi-2\varphi_0)=J^{-1/2}, \qquad (5)$$

where Φ is the phase of the driving field $E=I^{1/2}\exp(\mathrm{i}\Phi)$, and we have introduced the following dimensionless parameters describing the relative cavity detuning and the driving field intensity:

$$d\equiv\frac{\Delta}{\gamma}, \qquad J\equiv\left(\frac{k}{\gamma}\right)^2 I. \qquad (6)$$

The threshold value of J is

$$J_t=1+d^2. \qquad (7)$$

The zero-amplitude solution is stable in the region $J<J_t$, whereas the above-threshold solution is stable in the region $J>J_t$ for the case $d<0$ and in the region $J>1$ for the case $d>0$. Hence, we find a bistable behavior of n_0 versus J in the case of positive detunings. Note that in the bistability regime the unstable bunch of the steady-state intensity is described by Eq. (4) with a minus sign before the term $(J-1)^{1/2}$. Examples of the curves for the normalized semiclassical intensity $(\chi/2\gamma)n_0$ are represented in Fig. 1.

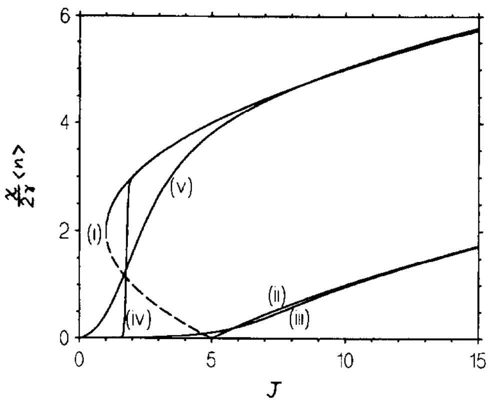

Fig. 1. The normalized mean intensity of the signal mode $(\chi/2\gamma)\langle n\rangle$ plotted against the pump intensity parameter J. Curves (i) and (ii) are related to the semiclassical result $(\chi/2\gamma)n_0$ for the cases $\Delta/\gamma=2$ and $\Delta/\gamma=-2$, respectively. The broken part of the curve (i) describes the unstable steady-state solution. Curves (iii)–(v) represent the exact quantum mechanical result for: $\Delta/\gamma=-2$, $\chi/\gamma=0.1$ (iii); $\Delta/\gamma=2$, $\chi/\gamma=0.1$ (iv); $\Delta/\gamma=2$, $\chi/\gamma=2$ (v).

It should be pointed out that occurrence of the stable above-threshold regime of oscillation in the undepleted pump approximation becomes possible due to addition of anharmonicity (self-phase modulation) to the parametric oscillator model Hamiltonian. The self-phase modulation changes the phase of the generated signal mode and hence destroys the phase matching condition for subsequent parametric $\chi^{(2)}$-interaction. This prevents the nonstationary increase of the signal intensity beyond the threshold and makes the parametric amplification inefficient. As a result of such a cancellation, the signal mode intensity becomes stabilized at a value determined by Eq. (4).

4. Exact quantum mechanical results and discussion

Now we shall give the results of the exact steady-state analysis of our nonlinear system. This analysis is based on the steady-state solution of the

Fokker–Planck equation (2) and on a calculation of various moments of the signal-mode operators by means of Eq. (3). Our study will include also an analysis of the photon number probability distribution function $p(n)=\langle n|\rho|n\rangle$, which is expressed in terms of the complex P-representation as follows:

$$p(n)=\frac{1}{n!}\int_C\int_{C'}\mathrm{d}\alpha\,\mathrm{d}\beta\,\alpha^n\beta^n\,\mathrm{e}^{-\alpha\beta}P(\alpha,\beta). \tag{8}$$

The exact steady-state solution of the Fokker–Planck equation (2) can be found using the method of potential solutions [1,23]. This yields

$$P_s(\alpha,\beta)=N(\chi\alpha^2+2kE)^{\lambda}(\chi\beta^2+2kE^*)^{\lambda^*}\times\exp(2\alpha\beta), \tag{9}$$

where

$$\lambda=-1-\frac{2\Delta}{\chi}-\mathrm{i}\frac{2\gamma}{\chi}, \tag{10}$$

and N is the normalization constant.

Substituting solution (9) into (3) and expanding the exponential term we find that the contour integrals are identical to those in the definition of the beta-function [24]. Thus we obtain

$$\langle a^{+m}a^n\rangle=\frac{M_{mn}}{M_{00}}, \tag{11}$$

where

$$M_{mn}=\left(-\frac{2k}{\chi}E\right)^{n/2}\left(-\frac{2k}{\chi}E^*\right)^{m/2}\times\sum_{l=0}^{\infty}\frac{1}{l!}\left|\frac{4k}{\chi}E\right|^l\left[1+(-1)^{l+n}\right]\times\left[1+(-1)^{l+m}\right]\times B\left(\lambda+1,\frac{l+n+1}{2}\right)\times B\left(\lambda^*+1,\frac{l+m+1}{2}\right), \tag{12}$$

and $M_{00}=M_{m=0,n=0}$.

Similarly, for the photon number distribution (8) we obtain

$$p(n)=\frac{G_n}{n!M_{00}}, \tag{13}$$

where

$$G_n=\left|\frac{2k}{\chi}E\right|^n\sum_{l=0}^{\infty}\frac{1}{l!}\left|\frac{2k}{\chi}E\right|^l\left[1+(-1)^{l+n}\right]^2\times B\left(\lambda+1,\frac{l+n+1}{2}\right)B\left(\lambda^*+1,\frac{l+n+1}{2}\right) \tag{14}$$

The results of the numerical calculations of the normalized quantum mechanical mean intensity of the signal mode $(\chi/2\gamma)\langle n\rangle$ ($\langle n\rangle=\langle a^+a\rangle$) versus J are represented in Fig. 1 for different values of dimensionless parameters $d=\Delta/\gamma$ and χ/γ. We see that whereas the semiclassical result exhibits hysteresis-cycle behavior in the case $d>0$ (curve i), the corresponding quantum mechanical result, which accounts for the influence of quantum noise, shows a gradual evolution. It is also seen that the characteristic threshold behavior, determined by a drastic increase of the intensity in the transition region, disappears as the relative nonlinearity χ/γ increases. Note that large values of χ/γ correspond to an increase of the quantum noise strength (see the diffusion terms in Eq. (2)). We note also that the semiclassical solution for $(\chi/2\gamma)n_0$ does not depend on χ/γ, in contrast to the quantum mechanical result.

Characteristic properties of threshold behavior are also seen from the analysis of the Fano parameter

$$F=\frac{\langle(\Delta n)^2\rangle}{\langle n\rangle}=1+\frac{M_{22}}{M_{11}}-\frac{M_{11}}{M_{00}}, \tag{15}$$

which describes dispersion of photon number fluctuations $\langle(\Delta n)^2\rangle=\langle n^2\rangle-\langle n\rangle^2$, normalized to the level of fluctuations for coherent fields $\langle n\rangle$. For small values of χ/γ, the Fano parameter has a well-localized sharp peak in the transition region, showing a critical increase of fluctuations (see Fig. 2). Its location can be identified with quantum mechanical "threshold", however, the peak becomes both smaller and broader as χ/γ increases, and hence the threshold is no longer well defined for increasing strength of quantum noise.

Analysis of the Fano parameter shows also the occurrence of the nonclassical effect of reduction of photon number fluctuations below the coherent level ($\langle(\Delta n)^2\rangle<\langle n\rangle$), i.e. it shows the formation of sub-Poissonian photon statistics. This effect occurs

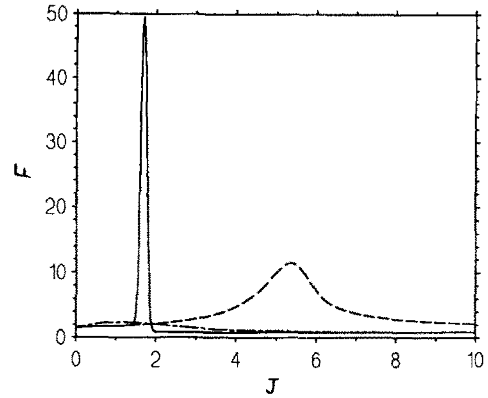

Fig. 2. Dependence of the Fano parameter F on J for: $\Delta/\gamma=2$, $\chi/\gamma=0.1$ (full curve), $\Delta/\gamma=2$, $\chi/\gamma=2$ (dotted curve); $\Delta/\gamma=-2$, $\chi/\gamma=0.01$ (broken curve).

beyond the threshold region and in the case $d>0$. The effect of reduction is destroyed with the increase of χ/γ and it is increased with the increase of d. For example, in the case $d=2$ and $\chi/\gamma=0.1$ the minimal value of the Fano parameter is $F\approx 0.81$, while in the case $d=10$ and $\chi/\gamma=0.1$ this value decreases to $F\approx 0.61$. Far above the threshold the photon number fluctuations become $\langle(\Delta n)^2\rangle \approx \langle n\rangle$.

Another quantum statistical characteristics we analyze is the normalized second-order correlation function

$$g^{(2)}=\frac{\langle a^+a^+aa\rangle}{\langle a^+a\rangle^2}=\frac{M_{22}M_{00}}{M_{11}^2}. \qquad (16)$$

Although the $g^{(2)}$-function is connected with the Fano parameter by a simple relation $g^{(2)}=1+(F-1)/\langle n\rangle$, it shows, however, some peculiarities (see Fig. 3). In particular, the sharp peak in the threshold transition region occurs in the behavior of the $g^{(2)}$-function in the bistable regime ($d>0$) only, while such a peak is absent in the case $d<0$. We recall that in contrast to this, the peak in the Fano parameter occurs in the threshold region for both cases $d>0$ and $d<0$. Hence the peaked behavior of the $g^{(2)}$-function is not just a direct reflection of enhanced photon number fluctuations, but is connected with the bistability phenomenon.

In the below-threshold region the $g^{(2)}$-function shows superbunching ($g^{(2)}\gg 1$), reflecting the pair creation of photons in the process of parametric down conversion. Above the threshold region and in the case $d>0$ we find a small amount of nonclassical effect of photon antibunching ($g^{(2)}<1$), which disappears ($g^{(2)}\to 1$), however, with the increase of J.

More detailed information on the quantum statistical properties of the signal mode can be obtained from the analysis of the photon number probability distribution function $p(n)$. Examples of curves for the $p(n)$-function are plotted in Fig. 4. In correspondence with the bistable behavior of the semiclassical steady-state intensity in the case $d>0$, we find a bimodal (double-peaked) structure of $p(n)$ in the transition region. This bimodal structure becomes, however less pronounced with the increase of χ/γ, i.e. with the increase of the quantum noise level. As is known (see, e.g., Ref. [25]) the locations of extrema of the $p(n)$-function, i.e. the locations of the most and least probable values of n, may be identified with the semiclassical stable and unstable steady states in the limit of small quantum noise level ($\chi/\gamma\ll 1$). With the increase of χ/γ, due to the multiplicative character [26] of the noise in our nonlinear system, the curve of locations of these extrema as depending on J becomes shifted from the corresponding semiclassical curve for n_0 (see Fig. 5). Another interesting result in the behavior of the $p(n)$-function consists in the possibility of coexistence of two local maxima even in the case $d<0$ (see Fig. 4b), when the semiclassical steady-state intensity is always monostable. In this case the corre-

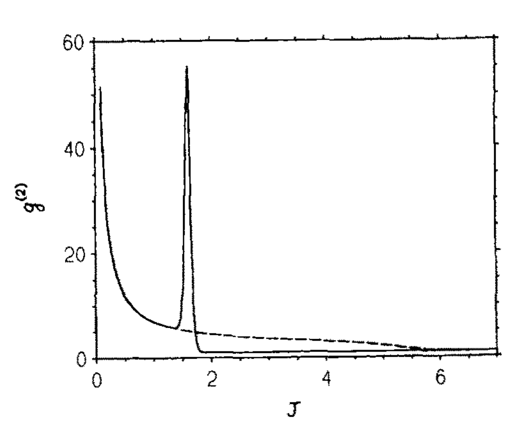

Fig. 3. Second-order correlation function $g^{(2)}$ plotted against J for: $\Delta/\gamma=2$, $\chi/\gamma=0.1$ (full curve); $\Delta/\gamma=-2$, $\chi/\gamma=0.01$ (broken curve).

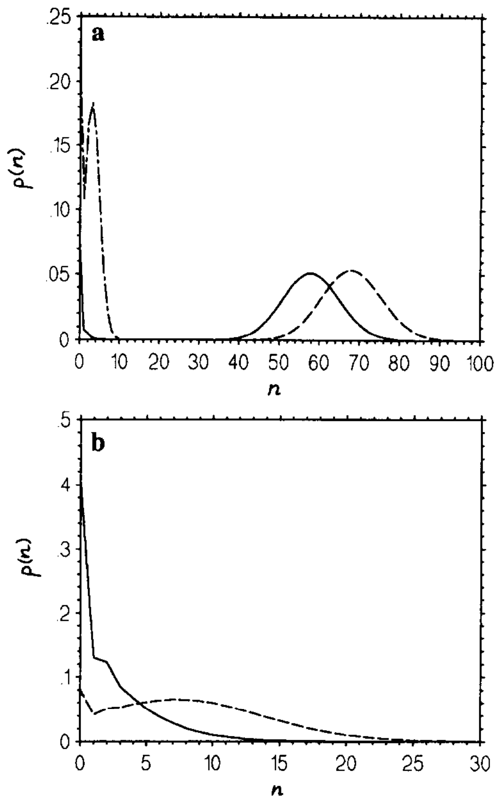

Fig. 4. Photon number distribution function $p(n)$. (a) Case $\Delta/\gamma = 2$ with $\chi/\gamma = 0.1$, $J = 1.84$ (full curve), $\chi/\gamma = 0.1$, $J = 3$ (broken curve), $\chi/\gamma = 2$, $J = 3$ (dotted curve) (b) Case $\Delta/\gamma = -2$ with $\chi/\gamma = 0.1$, $J = 5$ (full curve), $\chi/\gamma = 0.1$, $J = 7.2$ (broken curve).

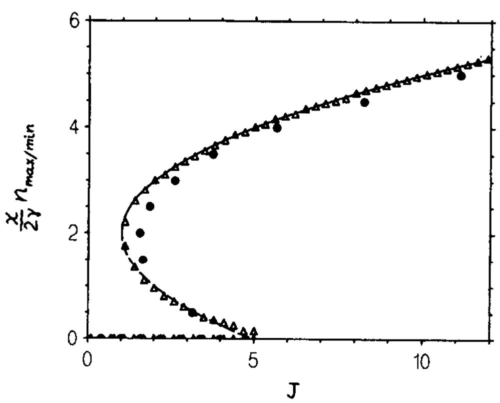

Fig. 5. Dependence of the most and least probable values of n in the $p(n)$-function (locations of the maxima and the local minimum) on J for the case $\Delta/\gamma = 2$ with $\chi/\gamma = 0.1$ (△) and $\chi/\gamma = 2$ (●). The curves are scaled by a factor $\chi/2\gamma$, and the corresponding semiclassical result for normalized intensity $(\chi/2\gamma)n_0$ is plotted for comparison.

spondence between the most probable values of n and the semiclassical steady state is absent. The transition from the shape of the $p(n)$-function with zero most probable n-value to the shape with nonzero most probable n-value, leading to an essentially nonzero mean intensity of the signal, takes place at the intensities J larger than the semiclassical threshold J_t.

Finally we present the result of the calculation of the minimal dispersion of fluctuations of the phase-dependent quadrature amplitude of the signal mode

$$\langle(\Delta X^{\theta})^2\rangle_{\min} = 1 + 2\left(\frac{M_{11}}{M_{00}} - \frac{|M_{02}|}{M_{00}}\right), \tag{17}$$

where $X^{\theta} = a\exp(-i\theta) + a^{+}\exp(i\theta)$ is the quadrature amplitude operator, with θ being the phase of the local oscillator. The dependence of $\langle(\Delta X^{\theta})^2\rangle_{\min}$ on J is represented in Fig. 6 for different values of d and χ/γ. We find that a nonclassical effect of squeezing of quantum fluctuations ($\langle(\Delta X^{\theta})^2\rangle_{\min} < 1$) occurs in our nonlinear system. A substantial reduction of fluctuations takes place in a wide region of J in the case of absence of bistability and for relatively small values of χ/γ. The maximal squeezing effect of about 50% is reached in the vicinity of threshold. In the bistable regime the squeezing effect occurs in the below-threshold region only. Note also that with the increase of χ/γ the squeezing is destroyed.

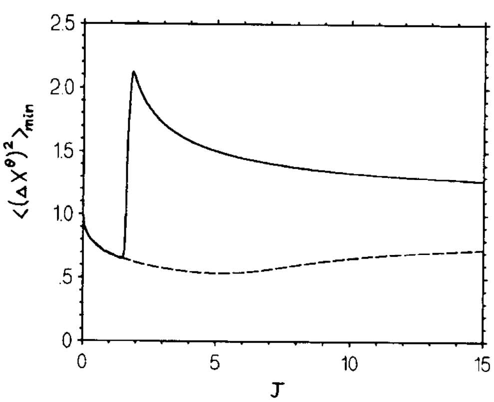

Fig. 6. Minimal dispersion of quadrature amplitude fluctuations $\langle(\Delta X^{\theta})^2\rangle_{\min}$ plotted against J for $\Delta/\gamma = 2$, $\chi/\gamma = 0.1$ (full curve) and $\Delta/\gamma = -2$, $\chi/\gamma = 0.1$ (broken curve).

References

[1] P.D. Drummond and D.F. Walls, J. Phys. A 13 (1980) 725.
[2] P.D. Drummond and C.M. Gardiner, J. Phys. A 13 (1980) 2353.
[3] P.D. Drummond, K.J. McNeil and D.F. Walls, Optica Acta 28 (1981) 211.
[4] G.J. Milburn and D.F. Walls, Optics Comm. 39 (1981) 401; Phys. Rev. A 27 (1983) 392.
[5] K.J. McNeil and C.W. Gardiner, Phys. Rev. A 28 (1983) 1560.
[6] G.J. Milburn, Phys. Rev. A 33 (1986) 674.
[7] G.J. Milburn and C.A. Holmes, Phys. Rev. Lett. 56 (1986) 2237.
[8] M. Wolinsky and H.J. Carmichael, Phys. Rev. Lett. 60 (1988) 1836.
[9] M.J. Collett and D.F. Walls, Phys. Rev. A 32 (1985) 2887.
[10] M. Kitagawa and Y. Yamamoto, Phys. Rev. A 34 (1986) 3974.
[11] Y. Yamamoto, S. Machida, N. Imoto, M. Kitagava and G. Björk, J. Opt. Soc. Am. B 4 (1987) 1645.
[12] B. Yurke and D. Stoler, Phys. Rev. Lett. 57 (1986) 13.
[13] P.D. Drummond and S.J. Carter, J. Opt. Soc. Am. B 4 1565.
[14] L.A. Wu, M. Xiao and H.J. Kimble, J. Opt. Soc. Am. B 4 (1987) 1465.
[15] M. Rosenbluh and R.M. Shelby, Phys. Rev. Lett. 66 (1991) 153.
[16] B. Wielinga and G.J. Milburn, Phys. Rev. A 48 (1993) 2494; 49 (1994) 5042.
[17] F. DiFilippo, V. Natarajan, K.R. Boyce and D.E. Pritchard, Phys. Rev. Lett. 68 (1992) 2859
[18] M.J. Werner and H. Risken, Phys. Rev. A 44 (1991) 4623.
[19] G.Yu. Kryuchkyan and K.V. Kheruntsyan, Quantum Semiclass. Optics 7 (1995).
[20] G.Yu. Kryuchkyan, K.V. Kheruntsyan, V.O. Papanyan and K.G. Petrossian, Quantum Semiclass. Optics 7 (1995).
[21] C.W. Gardiner, Handbook of Stochastic Methods (Springer, Berlin, 1986).
[22] W.H. Louisell, Quantum Statistical Properties of Radiation (Wiley, New York, 1973).
[23] H. Haken, Rev. Mod. Phys. 47 (1975) 67.
[24] D.S. Kuznetsov, Special Functions (Vysshhaya Shkola, Moscow, 1965) [in Russian].
[25] L.A. Lugiato, in: Progress in Optics XXI, ed. E. Wolf, (North-Holland, Amsterdam, 1984).
[26] W. Horsthemke and R. Lefever, Noise-Induced Transitions (Springer, Berlin, 1984).